Journal of Energy and Power Engineering 7 (2013) 1124-1131

Development of a Small Scale Magnetically Levitated Train as Demonstrator for Undergraduate Mechatronics Students

Rüdiger Appunn, Thomas Herold and Kay Hameyer

Institute of Electrical Machines, RWTH Aachen University, Aachen 52062, Germany

Received: July 04, 2012 / Accepted: November 16, 2012 / Published: June 30, 2013.

Abstract: At the Institute of Electrical Machines of the Rheinisch Westfälische Technische Hochschule Aachen University, there is a project financed by student fees for the realization of a magnetically levitated train in the scale of 1:50. Undergraduate students are supposed to get the possibility to design and build up a real train which serves as demonstrator for a mechatronic system. This project strengthens the motivation of students, since a practical demonstration of electromagnetic forces is given in addition to theoretical courses. This paper introduces the major project steps and explains the learning targets for the students. It focuses on analytical magnetic circuit design, numerical field simulation, modeling and control of a multi degree of freedom system, electronic circuit design, measurement setups and a first prototype test bench.

Key words: Electrical engineering education, magnetic levitation, modeling, control, finite element methods.

1. Introduction

The fascination for technology bases on its plasticity. To encourage the interest for electrical engineering, a small test bench for magnetic levitation is constructed, which is intended to be used at information events for pupils and visitors. It should be used for student demonstrations and laboratories as well. To provide a playful incentive the levitation train is designed on a scale of circa 1:50 (Fig. 1).

Small scale maglev trains for demonstration purpose can be found in literature in various papers. In Refs. [1, 2], design concepts of small scale maglev trains are introduced focusing on hybrid-excited magnetic levitation and drive topologies. The demonstrator train in Ref. [3] uses repelling forces created by a Halbach array of permanent magnets for levitation. Maglev vehicles using superconducting magnets for levitation or drive are presented in Refs. [4-7].

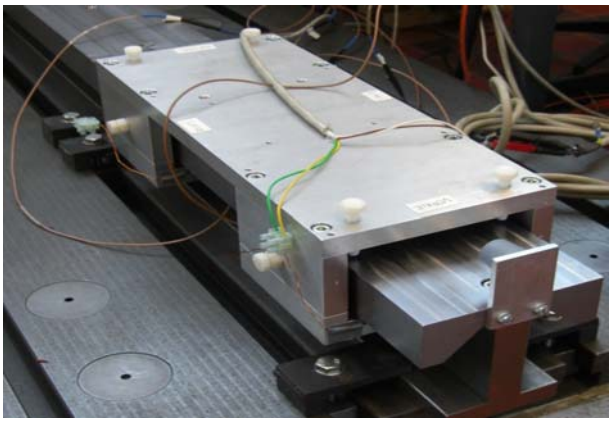

Fig. 1 Chassis of the magnetically levitated train on the test bench.

Magnetic levitation is a fascinating phenomenon; the motivation for undergraduate students is very high. In Refs. [7-11], magnetic levitation devices are used for education on control theory. Combined with a linear drive the experience is even more exciting as a contactless movement is enabled. Because of these points, a magnetically levitated train is selected as demonstrator for a mechatronic system. Other systems

Corresponding author: Rüdiger Appunn, research associate, research fields: magnetic levitation, linear guiding and contactless power supply. E-mail: ra@iem.rwth-aachen.de.

such as a controlled servo drive would not have the same attraction.

The educational expectations of this project are the modeling of a multi degree of freedom system, the development of a state space control, the commissioning in a rapid prototyping environment and later on the design of a linear drive and its control.

Magnetically levitated trains such as the Transrapid [12] in Germany or China and the Maglev [13] in Japan are well-engineered transport systems, which are partially in commercial operation.

2. Project Structure

The project is divided into numerous subprojects dealing with single design steps in the development of the small scale train. Student groups work on these projects and gather experience on many fields of electrical engineering. In the following several project steps are presented briefly.

2.1 Basic Concept

At the beginning of the project, a concept study is done. Here the basic principles for levitation and drive are evaluated. Different actuator and guide rail topologies are considered. The number of sensors and actuators required for a stable, contactless operation of the train is determined. Expected levitation and drive forces are appointed. Power supply and electronics are defined in this stage. A degree of freedom model of the train is developed and different control methods are evaluated. Exemplary the chosen guide rail topology is presented, here. The transrapid uses electromagnetic levitation, eight actuators in a c-topology (Fig. 2a) with four levitating actuators under the guide rail and four guiding actuators on the sides of the rail creating the attraction between train and rail. In contrast to the electrodynamic levitation, which is based on repulsion forces, an active guiding control is required to keep the air gaps constant. The guiding topology used for the demonstrator train, the so called half x-topology, is

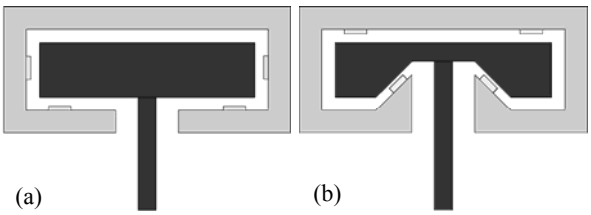

Fig. 2 (a) Guiding system c-topology (b) and half x-topology.

different. Hereby, four actuators are placed below the guide rail levitating the train. Due to the shape of the rail cross section the magnetic forces occur under a 45° angle. Fig. 2b depicts the cross section. This means that levitation and guidance are no longer separated and has to be decoupled by control strategies. The train has to be stabilized in five DOF (degrees of freedom), two lateral directions and three rotational around the axis of a Cartesian coordinate system. The last DOF, the driving direction, is controlled by the drive itself and no part of the linear guiding. Since 5° of freedom can not be controlled by four actuators, two additional actuators are placed on top of the guide rail. Now, six actuators control 5° of freedom.

2.2 Magnetic Circuit Design of the Levitation Actuators

Another part of the project is the electromagnetic design of the levitation/guiding actuators. Starting from analytical magnetic circuit models a numerical design of the actuators is done by students. To reduce the power compensation of the train, hybrid actuators [14], consisting of permanent magnets and coils are used. The actuators are dimensioned to compensate the weight of the train utilizing the offset force, created by the permanent magnets. With the coils around the lateral arms of the u-shaped yoke the pulling force can be adjusted. In Fig. 3, the flux density in the iron yoke is presented as part of the design stage.

2.3 Actuator Build-up and Measurements

The construction of the actuators is done in this project. The iron yoke is fabricated from laminated steel at the tool shop of the Institute of Electrical Machines. Hereafter students wind the coils around the

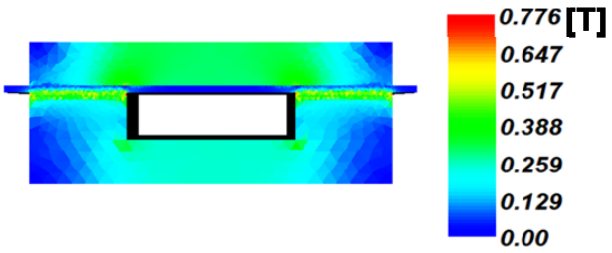

Fig. 3 Flux density [T] of the actuator resulting from permanent magnets.

lateral arms of the actuators and glue the permanent magnets on top the pole areas. Fig. 4 shows the actuator during the construction phase without permanent magnets. After construction the actuators are measured at a single actuator test bench. Fig. 5 depicts the test bench. The students have to consider a measurement setup and learn to measure non electrical quantities such as pulling forces. The measured forces of the actuators at different currents are shown in Fig. 6. At the nominal air gap of 1.5 mm the offset force resulting from the permanent magnets has been measured to 60 N. Due to the 45° angle of force application in x and y direction a force of

$$F_x = F_y = F_{actuator} \cdot \cos(45^\circ) = \frac{F_{actuator}}{\sqrt{2}} \quad (1)$$

is developed.

The four hybrid actuators can lift a total weight of 170 N at zero current.

2.4 Modeling

The dynamic system model is developed in this project part. Two possible control strategies are considered for the levitation and guidance of the train. At first an air gap control [15, 16], in which each of the six actuator air gaps is controlled independently, can be utilized. Applying this method six controllers are used and the strategy is less robust considering construction tolerances. The other control strategy is a degree of freedom control [17, 18]. Here, the five aforementioned DOF are controlled resulting in a more robust levitation as the air gaps are no longer coupled by the frame of the train. A transformation of local air gaps to global DOF has to be developed.

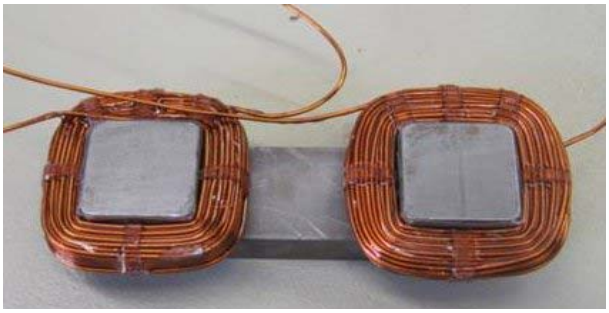

Fig. 4 U-shaped hybrid actuator without permanent magnets.

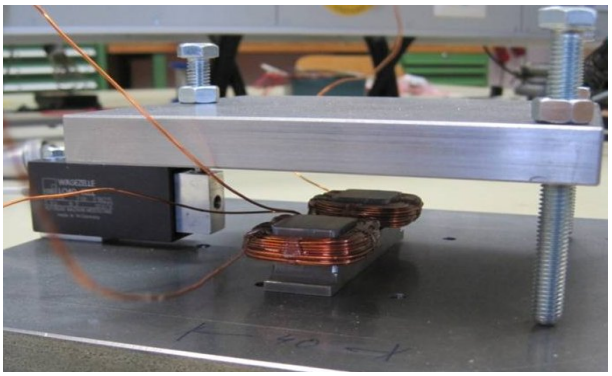

Fig. 5 Test bench for measuring of pulling forces.

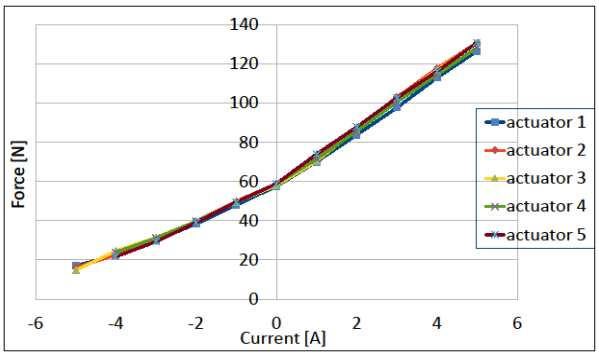

Fig. 6 Measured forces of the hybrid actuators.

Local quantities: The u-shaped hybrid actuators create pulling forces which are proportional to the square of the current I and inverse square of the air gap δ. For modeling purpose the pulling forces are linearized in a fixed working point of $\delta = 1.5$ mm and zero coil current. Eq. (2) indicates the linearization of the forces.

$$\begin{aligned} \vec{F}_{actuator} &= \vec{F}_{actuator}(\Delta\delta_N, I_N) \\ &+(\Delta\delta - \Delta\delta_N) \times \frac{\partial \vec{F}_{actuator}(\Delta\delta_N, I_N)}{\partial \Delta\delta} \\ &+(I - I_N) \times \frac{\partial \vec{F}_{actuator}(\Delta\delta_N, I_N)}{\partial I} \end{aligned} \quad (2)$$

Since the derivatives are constant, the linearization factors k_s and k_I can be introduced. In the working point $\Delta\delta_N = 0$ and $I_N = 0$. The attractive force $\vec{F}_M$ on the guide rail now depends linearly on air gap and current and in the case of the four hybrid magnets on the remanent force $\vec{F}_R$.

After linearization the local forces of the hybrid actuators can be described as:

$$F_{actuator,i} = k_s \times \Delta\delta_i + k_I \times I_I + F_R, i \in \{1;2;3;4\} \quad (3)$$

and the forces of two actuators without permanent magnets are:

$$F_{actuator,i} = k_s \times \Delta\delta_i + k_I \times I_I + F_R, i \in \{5;6\} \quad (4)$$

Global quantities: to simplify the modeling, the train is considered as mass point in the center of gravity of the construction. This leads to a constant weight of

$$F_g = m \times g \quad (5)$$

which the four hybrid actuators below the train have to counteract.

Beside lateral forces in x and y direction (see Fig. 7) the torque around the axis of a Cartesian coordinate system placed in the center of gravity as well:

$$\vec{M} = \vec{r} \times \vec{F} + I \times \vec{i}, i \in \{\alpha;\beta;\gamma\} \quad (6)$$

can act on the train. Where I is the inertia tensor.

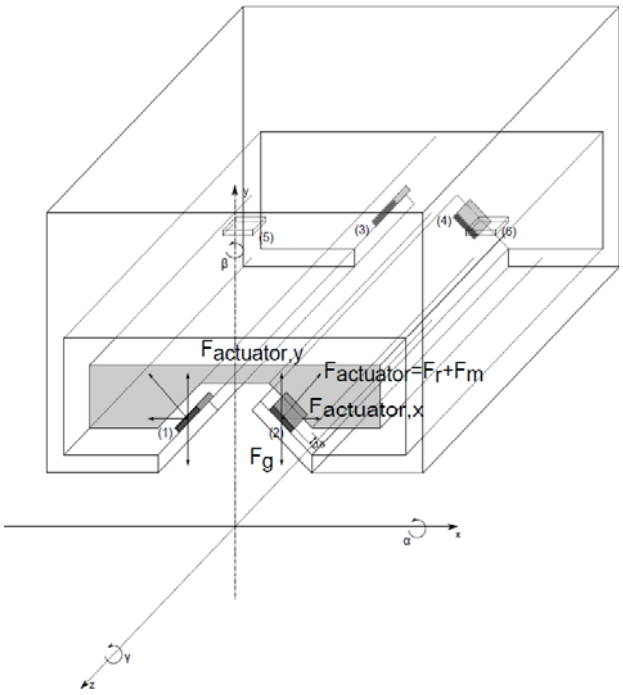

Fig. 7 Schematic description of the train.

The resulting force can be described as:

$$\vec{F} = m \times \vec{a} + m \times \vec{i} \times \vec{s}, i \in \{\alpha;\beta;\gamma\} \quad (7)$$

A vector can be defined including all global forces and torque:

$$F_{global} = \begin{pmatrix} F_x & F_y & M_\alpha & M_\beta & M_\gamma \end{pmatrix}^T. \quad (8)$$

The global air gaps, i.e. the DOF, are also summarized in a vector:

$$r_{global} = \begin{pmatrix} x & y & \alpha & \beta & \gamma \end{pmatrix}^T \quad (9)$$

$$\vec{F}_{global} = M \times \vec{r}_{global} \quad (10)$$

where M is the mass matrix.

$$M = \begin{pmatrix} m & 0 & 0 & 0 & 0 \\ 0 & m & 0 & 0 & 0 \\ 0 & 0 & J_x & 0 & 0 \\ 0 & 0 & 0 & J_y & 0 \\ 0 & 0 & 0 & 0 & J_z \end{pmatrix} \quad (11)$$

The mass and inertia tensor consist only of elements on the main diagonal, as the force application point the center of gravity equals the reference point of the coordinate system. Hereby deviation torque does not exist.

Coupling of local and global quantities: a mathematical model has to be defined, in which the transformation of local to global quantities is described.

The position of the actuators can be seen in Fig. 7. If a positive force F_x is applied to the train, the air gaps 1 and 3 become larger and air gaps 2 and 4 decrease. The Eq. (12) describes this correlation.

$$x = \frac{1}{4\sqrt{2}} \times (\Delta\delta_1 - \Delta\delta_2 + \Delta\delta_3 - \Delta\delta_4) \quad (12)$$

Opposite forces acting on different sides of the train result in a rotation.

Similar correlations can be found for the other DOF leading to the transformation matrix $T_{lg,gap}$:

$$T_{lg,gap} = \frac{1}{\sqrt{2}} \begin{pmatrix} \frac{1}{4} & -\frac{1}{4} & \frac{1}{4} & -\frac{1}{4} & 0 & 0 \\ -\frac{1}{6} & -\frac{1}{6} & -\frac{1}{6} & -\frac{1}{6} & \frac{1}{6} & \frac{1}{6} \\ \frac{1}{2\cdot a} & \frac{1}{2\cdot a} & -\frac{1}{2\cdot a} & -\frac{1}{2\cdot a} & 0 & 0 \\ \frac{1}{2\cdot a} & -\frac{1}{2\cdot a} & -\frac{1}{2\cdot a} & \frac{1}{2\cdot a} & 0 & 0 \\ 0 & 0 & 0 & 0 & -\frac{\sqrt{2}}{b} & \frac{\sqrt{2}}{b} \end{pmatrix} \quad (13)$$

The force and current transformation matrices can be defined using similar transformations.

2.5 State Space Control

Based on the mathematical modeling, the system description in state space is deduced from the differential equations.

As state values for every DOF the displacement x (potential energy) and the speed $\dot{x}$ (kinetic energy) are chosen. Additionally, the state space vector is enhanced by the integral of the displacement $\int x$. Hereby the system gets an integral character so that stationary displacements can be controlled. After transforming the linearized force equations the state space system is obtained:

$$\underbrace{\begin{pmatrix} x \\ \dot{x} \\ \ddot{x} \end{pmatrix}}_{\dot{x}} = \underbrace{\begin{pmatrix} 0 & 1 & 0 \\ 0 & 0 & 1 \\ 0 & -\dfrac{2\cdot\sqrt{2}\cdot k_s}{m} & 0 \end{pmatrix}}_{A_x} \cdot \underbrace{\begin{pmatrix} \int x \\ x \\ \dot{x} \end{pmatrix}}_{x} + \underbrace{\begin{pmatrix} 0 \\ 0 \\ -\dfrac{2\cdot\sqrt{2}\cdot k_I}{m} \end{pmatrix}}_{B_x} \cdot \underbrace{I_x}_{u} \tag{14}$$

$$y = \underbrace{\begin{pmatrix} 0 & 1 & 0 \end{pmatrix}}_{C_x} \cdot \underbrace{\begin{pmatrix} \int x \\ x \\ \dot{x} \end{pmatrix}}_{x} \tag{15}$$

Here, k_s and k_I are linearization factors. These two equations are the description of the uncontrolled system. A_x is the system matrix, B_x the input matrix, and C_x the output matrix. The feed through matrix D_x is chosen to be zero, since there is no direct feed through in a real system. Here, y is not the DOF y, but the output vector of the state space system. Fig. 8 shows the pole-zero plot of the uncontrolled DOF x, which depicts the eigenvalues of the system. It can be seen, that not all poles are placed in the negative half-plane, due to the negative stiffness of permanent magnets. Therewith, the system is unstable.

The entire DOF controller is designed with five parallel single state controllers. The system matrix is formed and with this the state space equation of the uncontrolled system is established. To stabilize the system, the poles of system matrix A_x have to be shifted.

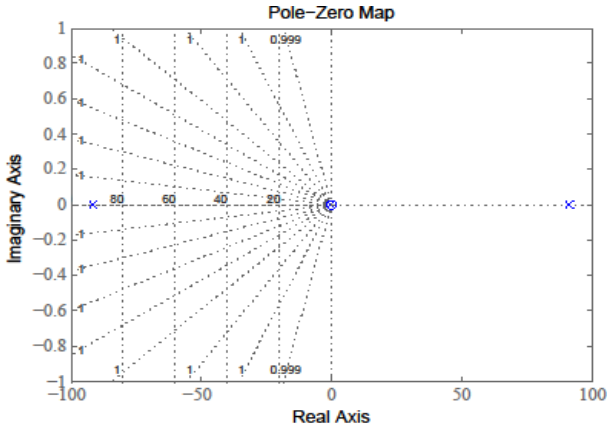

Fig. 8 Pole zero map of the uncontrolled system.

The eigenvalues are adjusted by a feedback of the state vector and a combination with the vector of the input values u.

Therefore, a control matrix K_x is introduced. It contains the control parameters, one for each state variable. The controlled system is shown in Fig. 9 and described by the following equations:

$$\begin{aligned} \dot{x} &= A_x \cdot x + B_x \cdot u \\ u &= -K_x \cdot x. \end{aligned} \tag{16}$$

Substituting the latter in the former results:

$$A_K = A_x - B_x \cdot K_x \tag{17}$$

with A_K as the system matrix of the controlled system.

The control parameter are first computed by Riccati equation design rules [19] and afterwards varied by pole placement. These rules are based on a minimization of a squared control quality measure. For the control parameter optimization, the method of pole placement [19] is used. This method is presented in several publications. In Ref. [17, 20], the use of this procedure is specified for the application in magnetic levitation controllers. Ghersin et al. [21] describes the pole placement for a 6-DOF vehicle. Other papers (e.g., Ref. [22]) show the implementation of the pole placement for other purposes. The controllers for the other four DOF are established the same way.

2.6 Simulation

In a first instance, the validity of the DOF-control is verified by a dynamic simulation with Matlab/Simulink. Several realistic and worst-case load

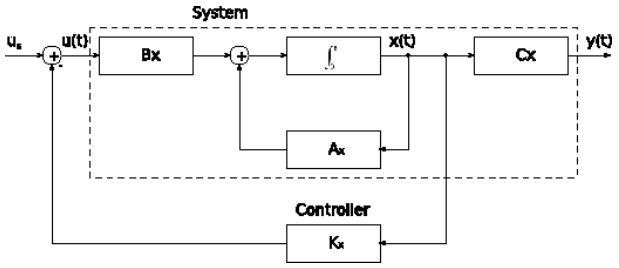

Fig. 9 State space model describing the train.

cases are computed, as well as the stiffness of the guiding system. A couple of force impacts on different positions of the train simulate disturbances during operation. In Fig. 10, a force impulse of 100 N applied in x-direction at 0.1 s is shown. The left air gaps (a, b) increase while the right air gaps (c, d) decrease. After a slight over shoot with a peak displacement of 22 µm the train resumes to its nominal position. The oscillation at the start of the simulation results from the initialization process since the weight of the train and the remanent force of the magnets do not compensate each other completely in parking position. The system response shows a robust guiding characteristic, even under extreme force impacts.

2.7 Mechanical and Electrical Prototype Build-up

The first prototype test bench consists of a 3 m long guide rail with the magnetically levitated train in scale of 1:50, compare Fig. 1. The dimensions of the train are given in Table 1. The aluminum chassis contains the six actuators, six eddy current sensors and plastic screws functioning as safety bearing. The position sensors measure all local air gaps, which serves as input signals for the DOF control. All electronics are installed separately outside the train, so at this design state power and sensor cables are connected to the train. In later states all electronics and a battery will be installed on board, guaranteeing an autonomous operation. Fig. 11 gives a detailed view of the air gaps. Here, the rail profile and the aforementioned components can be seen. The DOF control operates on a dSPACE rapid prototyping platform [23]. The Simulink control model runs on this board. The air gap information from the sensors are the input signals and

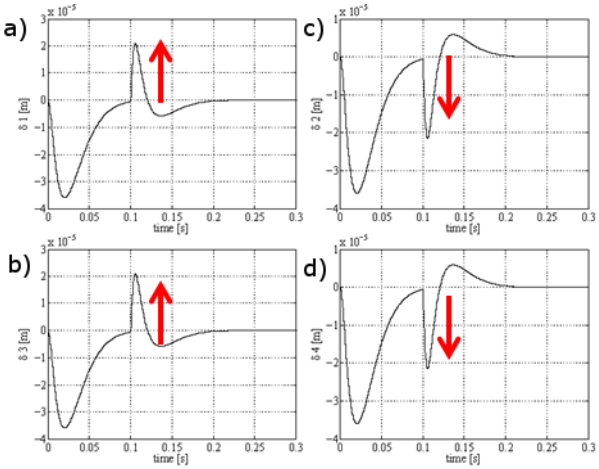

Fig. 10 Local air gap displacements resulting from force impact.

Fig. 11 Front view of the train depicting the sensors and actuators.

the output signals are the values of the coil currents. DC/DC converters operating at 25 kHz apply these currents to the actuator coils on the train. Fig. 12 depicts the scheme of the system.

2.8 Micro Controller Selection

In this project the students have to select a microcontroller platform on which the control will operate. Beginning with a definition of requirements, a market research is done. Hereafter a microcontroller is chosen and peripheral electronics is installed. Now all

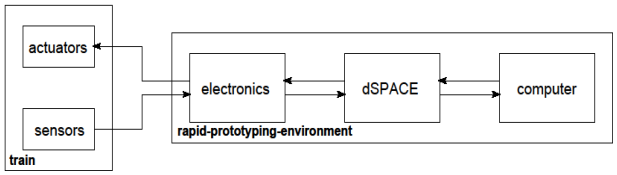

Fig. 12 Block-scheme representation of the full system.

control algorithms are implemented on the microcontroller and the system is put into operation. Fig. 13 depicts the circuit board.

2.9 Drive

The design of the linear drive is a further part of the project. The motor type is selected in this phase regarding the specifications for driving force and the limited space. Beginning from analytical designs a finite element model is built and numerical field computation is done for the fine design of the linear drive. Fig. 14 depicts an early design stage. After construction of a first drive prototype the motor has to be tested and put into operation.

3. Future Tasks

3.1 Integration of Electronics

In ongoing projects the power supply for the train and all electronics have to be integrated onboard the train. Students have to select suitable components and consider the limited space requirements to fulfill this task. Practical experience with electronic circuits is the main aspect of this project.

4. Conclusions

In this paper, an educational project is presented in which undergraduate students build up a magnetically levitated train in scale of 1:50. The working steps are presented exemplarily beginning from general topology considerations, the design of single components such as the actuators, measurements of these components to demonstrate their function, modeling and control and the build-up of a first prototype test bench. There is ongoing work for student projects till full operation of the train is achieved.

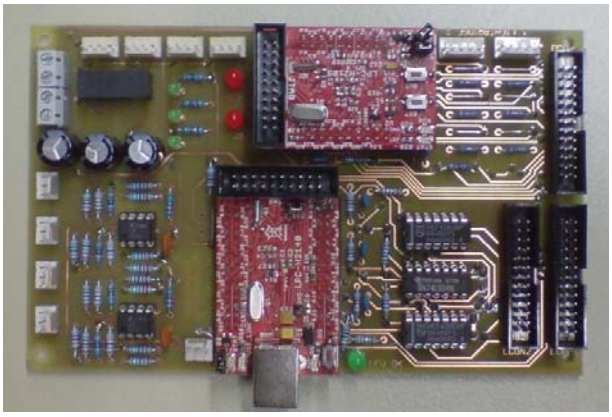

Fig. 13 Control circuit board.

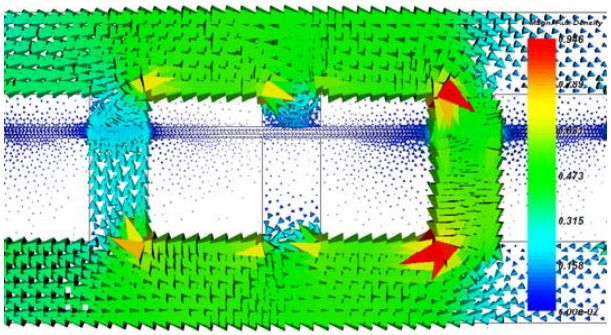

Fig. 14 Vectorial flux density [T] of the linear drive.

Table 1 Geometrical dimensions of the train.

Length *a* (mm)	500
Width *b* (mm)	200
Height *h* (mm)	123
Mass *m* (kg)	13.17

References

[1] H.W. Cho, C.H. Kim, J.M. Lee, H.S. Han, Design and characteristic analysis of small scale magnetic levitation and propulsion system for maglev train application, in: International Conference on Electrical Machines and Systems (ICEMS), Beijing, China, Aug. 20-23, 2011.

[2] C.H. Kim, H.W. Cho, J.M. Lee, H.S. Han, B.S. Kim, D.S. Kim, Levitation control of a hybrid-excited magnetic levitation vehicle, in: 11th International Conference on Control, Automation and Systems (ICCAS), Gyeonggi-do, South Korea, Oct. 26-29, 2011.

[3] R.F. Post, D.D. Ryutov, The Inductrack: A simpler approach to magnetic levitation, IEEE Transactions on Applied Superconductivity 10 (1) (2000) 901-904.

[4] R.M. Stephan, A.C. Ferreira, M.A. Neves, M.A.C. Moreira, M.A.P. Rosario, O.J. Machado, et al., A superconducting levitated small scale vehicle with linear synchronous motor, International Symposium on Industrial Electronics 1 (2003) 206-209.

[5] M. Ogata, K. Mizuno, Y. Arai, H. Hasegawa, T. Sasakawa, K. Nagashima, Trial manufacture of small HTS magnet using 2G tapes for maglev train application, IEEE Transactions on Applied Superconductivity 21 (3) (2011) 1556-1559.

[6] F. Yen, S. Zheng, X. Chen, J. Li, Q. Lin, Y. Xu, et al., Superconducting excitation system of a small scale linear synchronous motor, IEEE Transactions on Applied Superconductivity 22 (3) (2012) 5201103.

[7] J.M. Watkins, G.E. Piper, An undergraduate course in active magnetic levitation: Bridging the gap, in: Proceedings of the 35th Southeastern Symposium on System Theory, Morgantown, USA, Mar. 18, 2003.

[8] M.B. Naumovic, Modeling of a didactic magnetic levitation system for control education, in: 6th International Conference on Telecommunications in Modern Satellite, Cable and Broadcasting Service, Nis, Yugoslavia, Oct. 3, 2003.

[9] C.A. Dragos, S. Preitl, R.E. Precup, E.M. Petriu, Magnetic Levitation System laboratory-based education in control engineering, in: 3rd Conference on Human System Interactions (HSI), Rzeszow, Poland, May 13-15, 2010.

[10] P.S. Shiakolas, D. Piyabongkarn, Development of a real-time digital control system with a hardware-in-the-loop magnetic levitation device for reinforcement of controls education, IEEE Transactions on Education 46 (1) (2003) 79-87.

[11] P.S. Shiakolas, S.R. Van Schenck, D. Piyabongkarn, I. Frangeskou, Magnetic levitation hardware-in-the-loop and Matlab-based experiments for reinforcement of neural network control concepts, IEEE Transactions on Education 47 (1) (2004) 33-41.

[12] J. Meins, L. Miller, W. Mayer, The high speed maglev transport system Transrapid, IEEE Transactions on Magnetics 24 (2) (1988) 808-811.

[13] K. Sawada, Development of magnetically levitated high speed transport system in Japan, IEEE Transactions on Magnetics 32 (4) (1996) 2230-2235.

[14] B. Schmülling, O. Effing, K. Hameyer, State control of an electromagnetic guiding system for ropeless elevators, in: European Conference on Power Electronics and Applications, Aalborg, Denmark, Sept. 2-5, 2007. EPE, September 2007, pp. 1-10.

[15] D. Li, H. Gutierrez, Precise motion control of a hybrid magnetic suspension actuator with large travel, in: 34th Annual Conference of Industrial Electronics, Orlando, Florida, USA, Nov. 10-13, 2008.

[16] A. Forrai, T. Ueda, T. Yumura, Electromagnetic actuator control: A linear parameter-varying (lpv) approach, IEEE Transactions on Industrial Electronics 54 (3) (2007) 1430-1441.

[17] J.V. Goethem, G. Henneberger, Design and implementation of a levitation-controller for a magnetic levitation conveyor vehicle, in: The 8th International Symposium on Magnetic Bearing, Mito, Japan, Aug. 26-28, 2002.

[18] T. Herold, A. Pohlmann, K. Hameyer, Mathematical description and control design for the simultaneous levitation and propulsion of a conveyor vehicle, in: IEEE International Electric Machines and Drives Conference, Miami, USA, May 3-6, 2009. IEMDC ’09, 2009, pp. 113 –118

[19] O. Föllinger, Regelungstechnik-Einführung in die Methoden und ihre Anwendung, (Control Theory–Introduction in Methods and Application), Hüthig Buch Verlag Heidelberg, Germany, 1994.

[20] Y.S. Lu, J.S. Chen, Design of a perturbation estimator using the theory of variable-structure systems and its application to magnetic levitation systems, IEEE Transactions on Industrial Electronics 42 (3) (1995) 281-289.

[21] A.S. Ghersin, R.S. Sánchez Peña, LPV control of a 6-DOF vehicle, IEEE Transactions on Control Systems Technology 10 (6) (2002) 883-887.

[22] A.R. Oliva, S.S. Ang, G.E. Bortolotto, Digital control of a voltage-mode synchronous buck converter, IEEE Transactions on Power Electronics 21 (1) (2006) 157-163.

[23] K. Meah, S. Hietpas, S. Ula, Rapid control prototyping of a permanent magnet DC motor drive system using dSPACE and mathworks simulink, in: Applied Power Electronics Conference, APEC 2007, California, USA, Feb. 25-Mar. 1, 2007.